Journal of Polymer and Biopolymer Physics Chemistry, 2020, Vol. 8, No. 1, 15-27
Available online at http://pubs.sciepub.com/jpbpc/8/1/2
Published by Science and Education Publishing
DOI:10.12691/jpbpc-8-1-2

Model Drug Release from Potato Starch-Starch Glycolate Microparticles and Films with and without Incorporated Nano-SiO_2

Fateh Eltaboni[1,*], Amira Alhodeary[1], Mona Ibrahim[1], Fawzia Ali[1], Aya Al Abdali[1], Nadin Al Farsi[1], Fatma Elshibani[2], Mohamed Ali Sharkasi[3]

[1]Chemistry Department, University of Benghazi, Benghazi, Libya
[2]Pharmacognosy Department, University of Benghazi, Benghazi, Libya
[3]Pharmaceutical Chemistry Department, University of Benghazi, Benghazi, Libya
*Corresponding author: feltaboni@gmail.com

Received June 03, 2020; Revised July 04, 2020; Accepted July 12, 2020

Abstract Mixing potato starch (PSS) with sodium starch glycolate (SSG) and silica nanoparticles (SiO_2) substantially controls its swelling and mechanical behavior. Therefore, starch-starch glycolate-based delivery systems may be suitable for regulated model drug delivery. This work aimed to examine the release of dye from starch micro-particles and films as a mimic study for the drug release from an excipient. Starch film was prepared in vitro using glycerol as a plasticizing agent in aqueous gelatinous solution containing different amounts of SSG in the presence and absence of SiO_2. UV-vis spectroscopic technique was used to investigate the release kinetics of a model drug-like compound (Crystal violet, CV) in phosphate buffer solution (PBS) pH 7.4 at 37 ^{o}C. The swelling and folding strength of films have showed the different sensitivities of the films to SSG content and incorporation of SiO_2. It has been determined that SSG's cross-linking capability plays a critical role in starch's mechanical and rheological properties. Release of cationic drug across the polymeric films was significantly higher than that of the physical mixtures of CV in PSS-SSG microparticles. A higher release percentage was detected for PSE-Si-CV than that of PSE-Si-CV-$SSG_{1\%}$. The mechanism for the release of drugs was found to obey quasi-Fickian and non-Fickian diffusion mechanism for the PSS-Si-CV and PSS-Si-CV-$SSG_{1\%}$ films.

Keywords: *starch films, microparticles, mechanical properties, crystal violet, release*

Cite This Article: Fateh Eltaboni, Amira Alhodeary, Mona Ibrahim, Fawzia Ali, Aya Al Abdali, Nadin Al Farsi, Fatma Elshibani, and Mohamed Ali Sharkasi, "Model Drug Release from Potato Starch-Starch Glycolate Microparticles and Films with and without Incorporated Nano-SiO_2." *Journal of Polymer and Biopolymer Physics Chemistry*, vol. 8, no. 1 (2020): 15-27. doi: 10.12691/jpbpc-8-1-2.

1. Introduction

In recent years, industry has worked to reduce dependence on oil-based fuels and products due to increased environmental consciousness [1,2]. This contributes to the research of alternative materials that are environmentally friendly to replace existing [1]. The enormous increase in plastic production and use in our lives led to high plastic waste generation. Because of problems in disposal, as well as strict regulations and standards for a healthier and safer environment, much of scientific work has been directed towards eco-friendly environmentally materials to solve the problems caused by plastic waste [1-10]. Many researchers are focusing on biodegradable materials with similar properties and low cost replacement of petro-based plastics [5,11-19]. The use of biodegradable starches from various sources to prepare films and coatings with different properties has been documented in several studies [12,13,15,16,19-23]. Back in the 1950s, amylose films were self-sportingly made with and without plasticization of glycerol and evaluated for their mechanical and barrier properties [24,25].

Starch is a polysaccharide-based material derived from renewable sources, the major sources are the cereals, maize, rice, and wheat and the root vegetables, cassava and potatoes. Filming properties of potato starch are better compared to those of other processed starch films [26], since amylose content of starch is responsible for its film forming property [27]. However, the use of potato starch with 80% of branched amylopectin poses many drawbacks in packaging - low moisture sensitivity, weak mechanical properties and low solubility [26]. Hydrophilic groups and nanoparticles were taken into account to improve the characteristics of potato starch film. In addition, pure native starch films are fragile compared to synthetic polymer films and typically have to be plasticized. Glycerol is the most efficient plasticizer would most closely match the polymer structure that they plasticize. Glycerol is therefore the plasticizer most widely used in starch films [28-32].

Starch film has been recently used to deliver medicinal drugs for colon and plastic surgery in the treatment of face and wounds is promising for a starch film made of biodegradable plasticizing agents [20]. Unfortunately, the production of starch films is therefore severely hindered by their weak mechanical and strong hydrophilic properties that cause an unavoidable reduction in drug release performance [20]. The best way to overcome these drawbacks is to modify the starch structure via blending with other polymers like carboxymethyl cellulose (CMC), polyacrylic acid (PAA), poly vinyl alcohol (PVA), polyethylene (PE), poly (lactic acid), cellulose, chitosan, carboxymethyl chitosan, lignin and xanthan gum which helps to improve the mechanical characteristics and the hydrophilic properties of starch [1,4,8,15,19,20,21,33,34,35]. The majority of synthetic polymers however are hydrophobic, forming thermodynamically inextricable suspensions of starch. Therefore, simple mixing will produce a film with a phase inharmoniousness and poor mechanical properties [36]. Sodium starch glycolate (SSG) is a good candidate modified natural polymer for the starch blending. Because of its polymeric structure and high molecular weight, it can serve as a filler and cross-linking agent in film production. SSG can improve the mechanical and barrier characteristics of starch-related films. The key downside of SSG as a blender is high hydrophilic conduct and swelling capacities [37,38]. Thus, the silica nanoparticles (SiO_2) could be added to starch blend in order to enhance the water resistance of film, i.e. lowering hydrophilic character, SiO_2 nanoparticles has previously shown to have a great affinity of starch in the solution and has been used to study the polysaccharide-mineral interaction by inductively coupled plasma mass spectrometry analysis (ICP−MS), fluorescence, turbidimetry and spectrophotometry techniques [39,40,41,42]. Silica nanoparticles is a kind of amorphous powder with a net molecular structure of three dimensions. Its molecular formula is SiO_{2-n}, with n varying between 0.4 and 0.8. Silica nanoparticles is easy to disperse among the polymeric chains because of its nano-size, large specific surface area, high surface energy, unsaturated chemical bonds and hydroxyl moieties on the surface [43]. Several studies suggested that nano particles can enhance and improve the performance of synthetic polymers such as polyimide and polyacrylamide (PAM) [44,45] but a few studies on nano silica-modified starch polymers has been issued [26,43]. Because of its multi hydroxy properties and high surface activity, silica nanoparticles can be used for starch film modification.

In the present research, we explored the impact on the creation of a drug release method for pharmaceutical use by combining two drug carriers PSS and SSG with silica nanoparticles. The goal of this paper was therefore to demonstrate the feasibility of preparing a PSS-Si-SSG blend film in which hydrogen bonds between carboxy groups on SSG and hydroxy groups on starch are expected to develop. We have looked at the contribution of SSG-based film systems to controlled release of drugs. Crystal violet (CV) used as an in-vitro model to analyze pathways for the release of drugs. Ultraviolet visible spectrophotometry (UV-vis) has been used to characterize film casting and the release of CV. The properties (films swelling and folding) have also been tested, and the drug model release mechanism has been tested. Finally, we elucidated the mechanisms of removing drugs.

2. Materials and Methods

2.1. Materials

All materials in this work was used without further purification unless was mentioned. Glycerol (Sigma), double distilled water (Laboratory), disodium hydrogen phosphate (Sigma), potassium metabisulfite (Fluka), sodium chloride (Sigma), hydrochloric acid (Sigma), crystal violet crystals (CV) (Clin-Tech), chloroform (Sigma), iodine (Fluka), acetic acid (Sigma), potassium iodide (Fluka), xylene (Sigma), potato (Solanum tuberosum) was collected from local market of Benghazi city (Libya), starch from potato, soluble (PSS) (Sigma-Aldrich), sodium starch glycolate potato starch based (SSG, Type A) (Anhui Sunhere Pharmaceutical Excipients Co., Ltd), colloidal silica, 30 wt. % suspension in H_2O with a particle diameter of 34.7±1.4 nm, surface area of 225 m^2/g, pH of 9.2 (1 wt% in water), density of 1.21 g/cm^3, and molecular formula of SiO_2 (Sigma-Aldrich).

2.2. Methods

2.2.1. Potato Starch Extraction

The potato starch extraction (PSE) was done as described by Xie et al. [46]. Briefly, fresh whole potatoes were collected, washed, skinned, weighed, cubed, soaked in potassium metabisulfite aqueous solution, then milled on a cutter and washed with double distilled water. Filtrate was gathered and kept in a glass beaker for a period. Then the supernatant was poured out onto the firm starch sheet. This step was frequently repeated until it became transparent to the supernatant. Finally, starch lump was picked up and dried at room temperature, until a constant weight was gained.

2.2.2. Quantification of Extracted Potato Starch

The yield of starch from potato was measured by its reaction with iodine. Starch and iodine form a dark-blue complex with an absorbance maximum at 600 nm [47]. In a 100 mL volumetric flask of double distilled water, weight of solid biomaterial collected was diluted. A 10 mL aliquot was combined with 2.0 mL 1 M acetic acid, 2.0 mL freshly prepared iodine reagent, and 86.0 mL double distilled water. The iodine reagent was prepared in a 100 mL volumetric flask by dissolving 200 mg of iodine and 2000 mg of potassium iodide in double distilled water. For all samples with a 1 cm path-length cuvette, the absorbance spectra from 400 to 800 nm was measured in a CECIL CE7400 spectrophotometer (Cambridge, UK) A typical curve for various concentrations of pure potato starch was plotted by taking the absorbance value at 600 nm.

2.2.3. Molecular Weight Determination

Weight average molecular weight (M_w) for commercials and extracted starches was determined by light scattering

intensities which were measured in the visible range in terms of turbidity which is defined as the total light scattered in all the directions. It is frequently measured as the light reduced by non-absorbing materials using a UV-vis spectrophotometer. The mathematical relationship between turbidity (τ) in cm^{-1} and transmittance (T) or scattering ratio (R_θ), also known as the Raleigh ratio because of the excess scattering of the polymer in solution when compared with that of the solvent in the solution at the angle θ , is given by Equation (1) [48,49]:

$$\tau = -\frac{\ln T}{b} = \left(\frac{16\pi}{3}\right) R_\theta \quad (1)$$

where b is the cuvette path-length equal to 1 cm.

Meanwhile turbidity depends on the loss of light because of scattering material, it could be mathematically linked to the molecular weight of that particles by applying the like Rayleigh scattering equation, as shown in Equation (2) [50]:

$$\frac{Hc}{\tau} = \frac{1}{M_w} + 2B_2c \quad (2)$$

where c is the concentration of polymer in g mL^{-1} of solution, M_w the weight average molecular weight in g mol^{-1}, and B is a constant for any solvent-polymer solution and depends on the degree of interaction between the solvent and the polymer molecules. H is a constant for a solvent-polymer solution and is given by Equation (3) [50]:

$$H = \frac{32\pi^3 n_0^2}{3N_A\lambda_0^4}\left(\frac{dn}{dc}\right)^2 \quad (3)$$

in which n_0 is the refractive index of the solvent, N_A is the Avogadro's Number in mol^{-1}, λ_0 is the wavelength of the incident light in cm, dn/dc is the refractive index increment for any solvent-polymer solution (change in refractive index with polymer concentration in mL g^{-1}). A plot of Hc/t versus polymer concentration results in a straight line with an intercept on the Hc/t axis equals $1/M_w$, the reciprocal of which gives the weight average molecular weight of the polymer [50].

2.2.4. Charring Temperatures of Starch Microparticles

Autoignition of starch microparticles was measured by pouring quantity of starch in a capillary tube and inserted inside the melting point apparatus (Gallenkamp). A thermometer was incorporated to the machine to monitor the temperature. Through the glass window powder sample was viewed to observe when it started changing color from white to dark brown. This temperature range was recorded as the charring temperature.

2.2.5. Gelatinization Temperature of Starch Suspensions

Gelatinization temperature for starch suspensions was determined as a procedure mentioned in the literature with slight modification [51]. Briefly, A flat-bottomed flask was filled with 20 wt % dispersion of the starch and placed in a hot water bath. With the assistance of a thermometer, the temperature range of when gelatinization began and when it was completed was recorded.

2.2.6. True Density of Starch Microparticles

The true density (ρ_{true}) of the starch powder was determined by fluid displacement according to a protocol published elsewhere [2,51]. The weight of a 50 mL empty density bottle was recorded and subsequently filled with xylene. The led was put and excess liquid wiped off, and the weight of that filled bottle (W_3) was recorded. Around 5 mL of the liquid was withdrawn from the bottle and replaced with 0.5 g of PSS or SSG (W_2). Once the liquid level was reestablished, the density bottle was stoppered and the weight of liquid and powder (W_4) was documented. The true density for each powder was then calculated using Equation (4):

$$\rho_{true} = \frac{W_2W_3}{50(W_2 - W_4 + W_3)}. \quad (4)$$

2.2.7. Carr's Compressibility Index

The bulk density (ρ_b) for the powder of tree polymers was determined by measuring the mass of the dry powder and the equivalent volume for PSS, SSG and PSE. About 5 grams of powder sample was poured in a graduated cylinder has a capacity of 25 mL with graduations marked every 0.5 mL and it has an accuracy of ± 0.5 ml at 20°C. The bulk density was calculated by dividing the mass of the powder by the volume occupied in the cylinder. For the tapped density (ρ_t), the cylinder was tapped vigorously by hand till no more alteration in volume happened [52]. Flowability of each powder was estimated in terms of Carr's index (CI) [53]. Since CI was calculated from the bulk and tapped densities of PSS, SSG and PSE powders as shown in Equation (5):

$$CI = \frac{\rho_t - \rho_b}{\rho_t} x100. \quad (5)$$

2.2.8. Hausner's Ratio

Hausner's ratio was measured as the ratio of tapped density to bulk density of the starch powder, as a described in Equation (6) [2]:

$$Hausner's\ ratio = \frac{\rho_t}{\rho_b}. \quad (6)$$

2.2.9. Angle of Repose

Angle of repose (θ) for powders was measured as described in the literature [2]. A funnel was held with its tip 3 cm above a 10 cm filter paper. The starch powder was permitted to flow through the funnel until the peak of the cone was formed and fairly touched the tip of the funnel. The mean radius (r), of the base of the powder cone was measured and the tangent of the angle of repose calculated by using Equation (7):

$$\theta = \tan^{-1}\frac{h}{r} \quad (7)$$

where h is the height of the mound of starch powder.

2.2.10. Moisture Content of Starch Microparticles

The moisture content of the starch powders was measured thermo-gravimetrically using four digits balance and thermometer. 1 g of starch powder was balanced and

spread out on the petri dish. The samples were dried at 105°C for till get a constant weight. The weight difference because loss of moisture was calculated and expressed as the percent moisture content [2].

2.2.11. Making Starch Films

The starch films were prepared according to procedure taken from literature, with slight modification [54]. Briefly, 0.025 grams of silica microparticles were suspended in distilled water for 60 minutes and left to rest overnight, then the suspension blended with 2 grams of potato starch (PSS) and sodium starch glycolate (SSG) with variation of 0 wt%, 0.1 wt%, and 1 wt%, then 2 gram of hydrochloric acid was added to ensure the complete dissolving of polymer, after that the solution was neutralized by adding 2 grams of sodium hydroxide, hence the solution was mixed with 2 grams of glycerol, and distilled water in order to complete about 34 grams of solution. After homogenization, this solution was heated at 70°C under stirring until gelatinous starch was formed. Same procedure was repeated with various amounts of SSG but in absence of silica. Similarly, dyed film of starch extracted from potato (PSE) was prepared but a 0.25 grams of crystal violet dye (CV) was added to the film when in vitro dye release study was carried out. According to the casting technique, a specific content of filmogenic solution was poured onto squared glass plates (10 x 10 cm^2) to obtain smooth, unbroken and constant thickness films of 100 μm. Finally, prepared films were dried in desiccator at room temperature for approximately 72 hours. The drying process was continued until a constant weight was obtained.

2.2.12. Film Swelling

Water uptake by the film was gravimetrically measured by remarking mass of the wet film M_w after soaking in water for 25 hours at 37°C. The percentage of water absorption was calculated using the Equation (8) [34]:

$$S = \frac{M_w - M_d}{M_d} x100 \quad (8)$$

Where S is the swelling ratio and M_d is the weight of initial dry film.

2.2.13. Film Density

For determining film density, samples of 1.5 x 1.5 cm were maintained in a desiccator with phosphorus pentoxide for 7 days and weighed. Hence, dry film densities were calculated by applying Equation (9) [55]:

$$\rho_{film} = \frac{M}{A\delta} \quad (9)$$

where, A is the film area (2.25 cm^2), δ the film thickness (cm), M the film dry mass (g) and ρ the dry film density in g cm^{-3}. The film density was expressed as the average of 3 determinations.

2.2.14. Optical Property

Opacity and UV barrier capacity were determined from the absorbance spectra (200-750 nm) recorded in a CECIL CE7400 spectrophotometer (Cambridge, UK), with air as reference. Films were placed on the internal side of a quartz spectrophotometer cell. Film opacity (AU nm) was defined as the area under the recorded curve determined by an integration procedure according to Passaretti *et al.* [6], and the standard test method for haze and luminous transmittance of transparent plastics recommendations (ASTM D1003-00).

2.2.15. Folding Endurance

Folding strength or flexibility is a method to evaluate the mechanical properties of a film. It was measured by continually twisting prepared film strip of 2 x 2 cm, at 180° angle of the plane at the same place until it was broken. The number of times that the film could be twisted up and down without breaking is the value of folding endurance for that film. Higher folding endurance value describes the more mechanical strength of a film [56].

2.2.16. Determination of Dye Entrapment

The dye content in PSE-CV film was determined using a method reported by Nair *et al.* [57]. 1 g of PSE-CV film was placed in a volumetric flask containing 50 mL of phosphate buffer and kept overnight. Then the suspension was diluted up to 100 mL by adding distilled water and filtered after vigorous shaking. Finally, the absorbance of the solution was measured using a CECIL CE7400 spectrophotometer (Cambridge, UK). The dye content was estimated according to the Beer-Lambert's law as shown in Equation (10):

$$C = \frac{A}{\varepsilon b} \quad (10)$$

where, C is the concentration of CV dye, A is the absorbance at 580 nm, and ε is the extinction coefficient for CV dye and was determined the integration for the area under curve of visible spectra of dye, steps are represented by Equations (11) and (12):

$$A_i = \frac{a_{up}}{\left(\sqrt{\pi} w_{fwhm}\right) / \left(2\sqrt{2\ln 2}\right)} \quad (11)$$

where A_i is the absorbance of 12.5 μM of CV solution, a_{up} is the area under peak, π = 3.14, and w_{fwhm} is the full width at the half maximum of peak. From the absorbance A_i, the absorption coefficient e is determined by Equation (12):

$$\varepsilon = \frac{A_i}{C_i b} \quad (12)$$

where b is the path length of sample in cm and C_i is the concentration at A_i value.

2.2.17. Physical Mixtures of Starch Microparticles

Physical mixtures of PSE and SSG microparticles used for comparison of release with the prepared films were prepared by gentle mixing of known quantities of CV and potato starch powder contain 0 % and 1 % of SSG with a ceramic mortar and pestle for 10 min. Then 50 mg of resulted mixture was applied for the release study.

2.2.18. In-Vitro Dye Release

In vitro dye release from PSE film was carried out according to a protocol taken from the literature with minor adjustments [57]. Dissolution study was done on a dissolution bath with a rotation speed of 50 rpm in a paddle type. The test was performed in 900 mL of freshly prepared phosphate buffer solution (PBS) pH 7.4. A weighed quantity of dye loaded film was placed in dissolution medium maintained at 37°C. The amount of drug released into the medium was determined by withdrawing 5 mL of the dissolution fluid at predetermined time intervals. The volume withdrawn was replaced immediately with an equal volume of release medium with the same temperature to maintain sink conditions. The absorption of withdrawn solutions was determined at 580 nm using a CECIL CE7400 spectrophotometer (Cambridge, UK) after filtration and suitable dilution. All determinations were done in triplicate.

2.3. Release Kinetic Models

There is variety of kinetic models, which defined the overall release of drug from the dosage forms. Because qualitative and quantitative alterations in a formula may additionally adjust drug release in vivo performance, growing tools that facilitate product improvement with the aid of reducing the need of bioresearch is always desirable. On this regard, using in vitro drug dissolution information to expect in vivo bio-performance may be taken into consideration because the rational improvement of controlled release method [58]. Herein four mathematical models were utilized to investigate crystal violet release kinetics which is explained below.

2.3.1. Zero Order Model

Zero order kinetic is used to fit the mechanism of constant drug release from a drug delivery system [58,59]. In order to investigate the drug release kinetics data gained from in-vitro dissolution study the cumulative drug release is plotted against time. In this model the slope gives the zero-order rate constant and the correlation coefficient of the plot will decide whether the drug release fits zero order kinetics or not [58,59]. As specified by the principles of pharmacokinetics, drug release from the dosage form might be measured by Equation (13):

$$Q_t = Q_0 + K_0 t \quad (13)$$

Where Q_t is the cumulative amount after time t, Q_0 is the initial amount of drug at time equal to zero, and K_0 is the zero-order rate constant in concentration per time units [58].

2.3.2. First Order Model

First kinetic model is applied to analyze the drug release in pharmaceutical dosage forms which contain water-soluble drugs in porous matrices [58]. The drug release which follows first order kinetics could be symbolized by Equation (14) [58,59]:

$$LogQ_t = LogQ_0 + \frac{K_1 t}{2.303} \quad (14)$$

where, Q_t is the amount of drug released in time t, Q_0 is the initial amount of drug and K_1 is first order constant. In this model the graphical representation of the log cumulative of % drug remaining release versus time will be linear with a slope equal to $K_1/2.303$. The dosage form obeys to this model includes those having water soluble drug in a porous matrix and release the drug that is directly proportional to the amount of drug released by unit of time [60].

2.3.3. Higuchi Model

In 1961 Higuchi established mathematical models to examine the release of water soluble and sparingly soluble drugs loaded in solid matrix [60]. The dissolution from a system containing a homogeneous matrix can be expressed by Equation (15):

$$Q = K_H t^{1/2} \quad (15)$$

where Q is the amount of drug released in time t per unit area of matrix, K_H is the Higuchi dissolution constant. Higuchi describes drug release as a diffusion process founded in the Fick's law. For diffusion-controlled process a plot of Q versus square root of time is linear with a slope equal to the Higuchi constant [60].

2.3.4. Korsmeyer-Peppas Model

Once it has been established that the key mechanism of drug release is diffusion controlled from Higuchi model then it comes the release of drug tracks which kind of diffusion [59]. To distinguish the dissolution mechanisms from a drug matrix, the release data should be fitted by means of the empirical model suggested by Korsmeyer and Peppas[59]. Korsmeyer and Peppas introduced forth a simple equation describes the drug release from a polymeric system and decides which sort of dissolution, the equation can be represented by Equation (16):

$$\log\left(\frac{M_t}{M_\infty}\right) = LogK_{KP} + nLogt \quad (16)$$

where M_t is the fraction of drug released in time t, M_∞ is the amount of drug released after time ∞, n is the diffusional or drug release exponent, K_{KP} is the Korsmeyer release rate constant. To explore release kinetics a logarithm of cumulative % drug release (log M_t/M_∞) against logarithm of time (log t). The slope which gives n value is used to classify different release mechanisms as given in Table 1 [61,62].

Table 1. Different Release Mechanisms

Release Exponent (n)	Drug Transport Mechanism	Rate as a Function of Time	Drug Release Mechanism
n < 0.5 (0.45)	Quasi-Fickian diffusion	t^n	Non swellable matrix-diffusion
n = 0.5 (0.45)	Fickian diffusion	$t^{0.5}$	
0.5 (0.45) < n < 1	Non-Fickian diffusion (Anomalous)	t^{n-1}	For both diffusion and relaxation (erosion)
n = 1 (0.89)	Case II transport	time -independent	Zero-order release
n > 1 (0.89)	Super case II transport	t^{n-1}	Relaxation / erosion

3. Results and Discussion

3.1. Quantification and Kinetics of Starch Extracted from Potato

Spectrophotometric method using iodine as a marker was a good protocol for a quantitative evolution of starch extracted from potato, as shown in Figure 1. The kinetic calculation for the potato experiment was done by weighing of 0.42 grams from fresh potato and average absorbance value was recorded as a function of time. From the linear regression analysis of y=5.102x+0.08508 the starch concentration was determined by rearranging the formula to x= (y- 0.08508)/5.102. For instance, after one hour of extraction the starch concentration was found to be 0.042 mg/mL. Sine the dilution factor was 1:10 making it a concentration of 4.2 mg/mL. This amount was extracted from 0.42 g of fresh potatoes. The total amount of starch in 1 g potatoes was therefore 10 mg or 1 % of the fresh weight. The extraction kinetic data of starch was mathematically fitted by plateau followed by one phase decay using GraphPad prism software®. The half-life of extraction was 4.21hours with R^2 equal to 0.9768, this suggested that the applied model was a proper fit to determine the time at which the half amount of starch is extracted from 1 gram of potato.

3.2. Characterization of Starch Microparticles

Plots of Hc/τ against PSS, PSE, and SSG concentration produced straight lines as shown in Figure 2. The weight average molecular weight (M_w) for each polymer which is the reciprocal of intercept is displayed in Table 2. The following values of dn/dc (in cm^3/g) were used in calculating polysaccharide molecular weights: PSS, 0.150(l = 589 nm) [63]; PSE, 0.150(l = 589 nm) [63]; and SSG, 0.154 (l = 436 nm) [64]. It can be noted that M_w values of PSS and SGG were in the range of molecular weight of polymer applicable as pharmaceutical excipients [37]. Also, starch extracted from potato (PSE) produced a weight average molecular weight close to the commercial starch. Table 2 also lists some physicochemical and powder properties of commercial and extracted starches are demonstrated. It was found that the pH extracted potato starches, PSE, (6.5) which is very close to the commercial starch, PSE, (6.8), and SSG was weak acidic (6), these acidity values fulfill the British Pharmacopoeia conditions of excipients [65]. Moreover, the moisture content of PSE, SSG, and extracted potato starch evaluated was within the limits (10-20%) recommended by the British Pharmacopoeia [65].

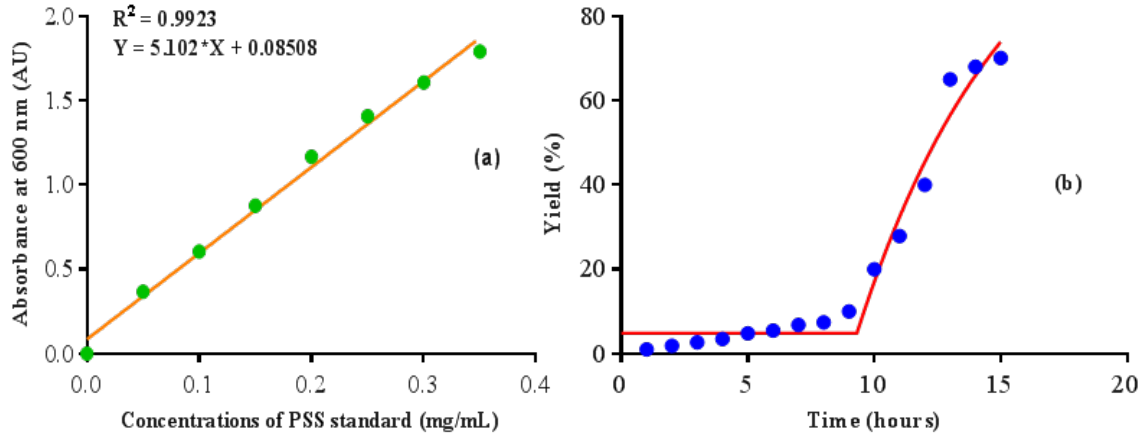

Figure 1. Standard curve for PSS solutions using absorbance at 600 nm (a). Kinetics for experimental data of starch yield per one gram of potato (dots) a combined with a mathematical fitting, plateau followed by one phase decay (solid lines)

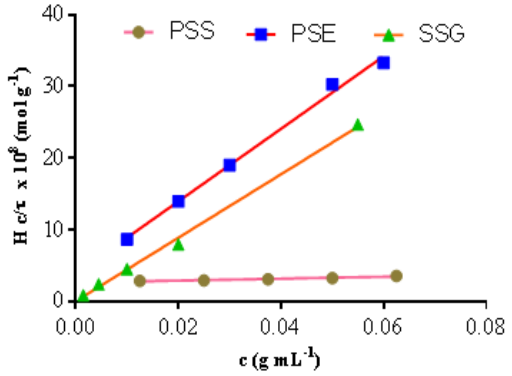

Figure 2. A plot of Hc/τ versus the concentration of PSS, PSE, and SSG polymers (R^2 for PSS = 0.9496, for PSE R^2= 0.9951, and for SSG R^2 = 0.9970)

Table 2. Physicochemical characterization of PSS, SSG, and PSE powders

Polymer powder / Property	PSS	SSG	PSE
$M_w x10^6$ (g/mol)	262	0.82	381
Particle size (μm)	10-100*	30-100*	-
Amylose content (%)	20-23*	-	-
Bulk density (g/cm^3)	0.6900	0.7453	0.7100
Tapped density (g/cm^3)	0.8500	0.9183	0.8720
True density (g/cm^3)	1.48	1.53	1.50
Carr's Index	18.82	18.84	18.58
Hausner's ratio	1.231	1.232	1.228
Angle of repose	36.93°	36.96°	36.84°
Moisture Content (%)	18	10	20
pH	6.8	6.0	6.5
Charring temperature (°C)	220-235	200-225	222-238
Gelatinization temperature (°C)	65-75	58-69	67-77

*As informed from the supplier.

SSG powder had higher bulk density (0.7453), tapped density (0.9183) and true density (1.53) compared to values of 0.6900, 0.8500 and 1.48 recorded for the PSS. Interestingly, density values of extracted potato starch (PSE) were very close to commercial one (PSS), as seen in Table 2. PSS and SSG powders evaluated had relatively similar mean particle size range (10-100 μm). This particle size distribution is acceptable for good excipient since fine powders (particle size < 75 μm) have poor flow which undesirably affect uniformity of the dosage unit and minimize their application in direct compressions [2]. The extracted potato starch like the commercial starches had good values for angle of repose (36.84^{o}), Hausner's ratio (1.228) and Carr's compressibility index (18.58) which confirmed their good flow properties (Table 2). The gelatinization temperature range of extracted potato starch was 67-78°C which agrees with the commercial starches, PSS and SSG (Table 2). This, gelatinous behavior of starches used in this work, correlates with the gelatinization temperature range of potato starch that reported in the literature (65-77°C). As it can be seen from Table 2 all starch powders do not melt, but autoignite above 200°C, this gives an idea of their thermal stability.

3.3. Characterizations of Starch Films

3.3.1. Optical Properties

After solvent casting, films had smooth surfaces and were dry, thin, flexible, transparent to cloudy, and free from bubbles. Dry films were simply detached from the glass mold (casting vessel), perhaps because of the existence of plasticizer. Under visual checkup, films were homogenous. However, when dye was loaded into films the films were colored. Thus, the optical properties were only carried out on the undyed films.

Figure 3 displays UV-vis spectra of PSS films and its composites, it is associated with UV barrier capacity and opacity in bar plots. Opacity values were applied to evaluate the effect of silica nanoparticles (SiO_2) and SSG on PSS films transparency. Mostly, in the circumstance of composites convey information about the filler size scattered inside the PSS matrix. Accordingly, molecule sizes bigger than visible wavelengths would scatter light, prompting cloudy films [6]. It was expected that PSS produces a film with a minimum opacity values, increasing gradually with adding SiO_2 and dramatically with addition of SSG in film composite formulations. The lowest opacity was a desirable property for PSS films to visualize the loading of model drug (CV). As shown in Figure 3 UV absorption of starch films was determined at a wavelength range from 250 nm to 300 nm. The UV barrier capacity of PSS films was slightly enhanced by increasing the amount of SSG, but no effect was observed upon adding silica.

3.3.2 Mechanical Properties

Folding endurance reflects the film's ability to bear breakage when repeatedly folded along the same path. High folding endurance values depict a considerable mechanical strength of the film [66]. It is directly regulated by the amount of plasticizer used in the formulation. The folding durability of the film was in order, PSS > PSS-$SSG_{0.1\%}$ > PSS-Si > PSS-Si-$SSG_{0.1\%}$ > PSS-$SSG_{1\%}$ > PSS-Si-$SSG_{1\%}$ (Figure 4). Folding endurance values of the produced films were found within acceptable range for oral films [66] and the highest folding strength occurred for PSS film (100 folds), indicating good strength and elasticity, which can be attributed to the use of the plasticizer which has property to add flexibility to films [66,67]. As a plasticizer, glycerol can reduce intermolecular forces between macromolecule bonds, enhance film flexibility and growth the elongation percentage [67]. Also, addition of glycerol into the film solution could result in numerous structural changes in polymer tissue, thus the film matrix becomes less rigid, the polymer chains shift, and the flexibility of the film increases [67]. This result fits with observation reported by Wahyuningtyas *et al. [67]* who found that adding of glycerol concentrations between 0-15% effects the mechanical characteristics of the carboxymethyl cellulose (CMC) - corn starch edible film, i.e. the reduction of the tensile strength in the range of 0.1405-4.7960 MPa and the increase in the percentage elongation of 30.21-313.99%. In this study the concentration of plasticizer was fixed at concentrations of 5% based on earlier reports which demonstrate good plasticization effect of propylene glycol [66]. Preliminary experiments (data not shown) indicated glycerol content of 5% as the best concentration. But, at higher concentrations cracked thick films were produced. However, incorporation of crosslinking and filler agent (SSG) in PSS-$SSG_{0.1\%}$ and PSS-$SSG_{1\%}$ films has decreased folding endurance to 90 and 80 folds, respectively; this observed decrease in flexibility with an increase in the concentration of SSG could be because of the increase in the degree of crosslinking of the polymeric chains which restricts the free movement of starch molecules. Likewise, the presence of SiO_2 nanoparticles lead to minimize folding endurance in PSS-Si, PSS-Si-$SSG_{0.1\%}$, and PSS-Si-$SSG_{1\%}$ films (85, 83 and 75 folds, respectively). This behavior was predictable and was credited to the resistance employed by the mineral itself and to the aspect ratio and orientation of the introduced silicate layers [36]. Additionally, the stretching resistance of the oriented backbone of the polymer chain in the film matrix linked by hydrogen bonding correspondingly contributed to declining the folding strength. The silica performances as a mechanical reinforcement of starch dropping the flexibility of the macromolecule [36]. The key purpose for this development in the mechanical properties is the stronger interfacial interaction between the film matrix and exposed surface of SiO_2 nanoparticles. Through the casting and drying of the films, the original hydrogen bonds formed between the hydroxyl groups in starch were swapped by the new hydrogen bonds formed between the hydroxyl groups in starch, the hydroxyl and carboxyl groups in SSG and the hydroxyl groups in hydrated silica. The existence of these new hydrogen bonds capable to enhance the mechanical properties.

3.3.3. Films Densities and Swelling Properties

Figure 4 shows density of control (PSS) and composite films (PSS-Si, PSS-$SSG_{0.1\%}$, PSS-$SSG_{1\%}$, PSS-Si-$SSG_{0.1\%}$, and PSS-Si-$SSG_{1\%}$). The density of PSS film was about 20 x 10^{-3} g/cm^3 this value reduced to half when silica nanoparticles were added in PSS-Si film, but by adding SSG to PSS the density of films was doubled in absence

of silica (PSS-SSG$_{0.1\%}$ and PSS-SSG$_{1\%}$ films). In contrast, a minimum reduction in the density values was recorded in presence of silica (PSS-Si-SSG$_{0.1\%}$ and PSS-Si-SSG$_{1\%}$ films). Figure 4 also represents water uptake by the films expressed in swelling percent (S). The films kept their integrity, precisely, they did not dissolve or cut up throughout the experiment. This is a supportive evidence for occurring successful crosslinking between PSS and SSG considering that SSG is soluble in cold water. It is worth to state that all the films after test visually returned to their original mass. Swelling ratio denotes to the water retentive capacity and depends on the existence of hydrophilic groups such as carboxyl, free volume besides crosslinking density [35,68]. It was observed that the PSS film swelled by 15%, then in absence of silica PSS-SSG films are more swelling than the control film, and the films conditioned at 1% SSG possessed higher swelling index than film in 0.1% SSG, since it reached its maximum at 67 % for PSS-SSG$_{1\%}$ film. On contrary, swelling power was reduced of PSS film when silica nanoparticles were added (that is, 7% S) had the half S of PSS film, while they contained 17% and 24% S for PSS-Si-SSG$_{0.1\%}$, and PSS-Si-SSG$_{1\%}$ films. However, film samples contain SSG were higher in swelling ability than native PSS film, which is the result of higher hydrophilic behavior of SSG when compared to PSS, what correlates with the water uptake results [68]. Whereas, the addition of silica reduced the films swelling as previously reported by Ismail *et al.* [21], which could be attributed to the network created by blending silica nano particles with potato starch films, this might improve the water resistance and inhibit the solubility of the films [21,23]. Hence, combining starch with silica led to a reduction in the water absorption of films. Moreover, the water absorption capability acts as a vital property, especially for oral thin films. As reported by previous study [69], that the film containing 2% w/v of both sodium carboxymethylcellulose and hydroxyethyl cellulose, exhibited good swelling index (31%), a suitable residence time and promising controlled drug release, therefore could be nominated for the development of oral thin films for effective therapeutic usages.

Based on swelling and hydrophilicity of SSG, PSS-Si-SSG$_{1\%}$ were selected for *in vivo* model drug release study and PSS-Si was used as a control. Building on the similarity in physicochemical behavior for both commercial and extracted potato starches (see Table 2), PSE was chosen for investigating the release behavior of crystal violet dye (as model drug). Figure 5 shows the physical appearance of dyed and undyed starch films.

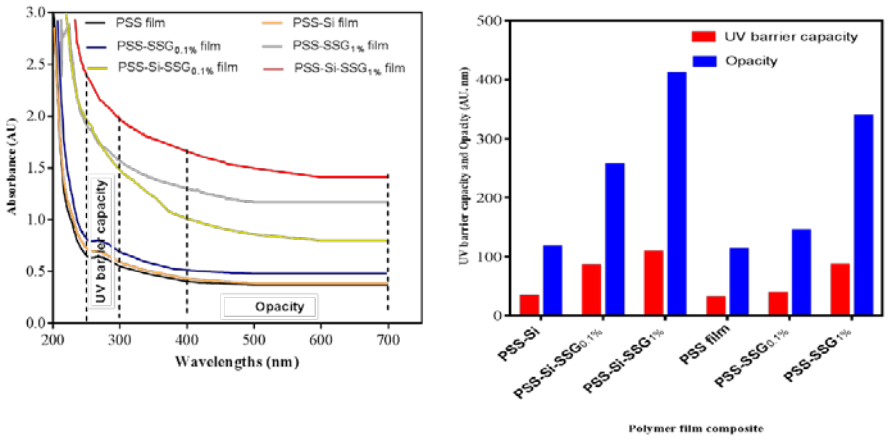

Figure 3. Absorption spectra, opacity (blue bars), and UV-barrier capacity (red bars) of potato starch soluble film (PSS), PSS with silica film (PSS-Si), PSS with 0.1 % of starch glycolate film (PSS-SSG0.1%), PSS with 1 % of starch glycolate film (PSS-SSG1%), PSS with silica and 0.1 % of starch glycolate film (PSS-Si-SSG0.1%), and PSS with silica and 1 % of starch glycolate film (PSS-Si-SSG1%)

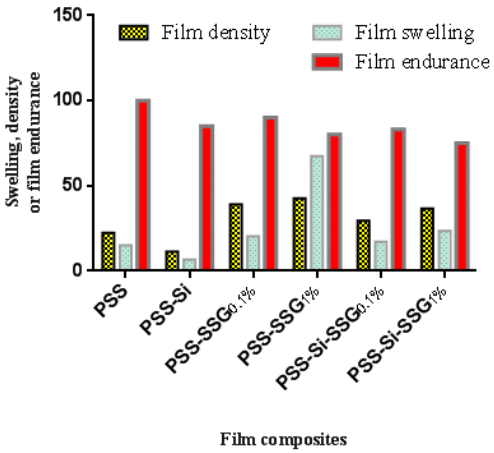

Figure 4. Densities (ρ_{film} x 10^{-3} g cm^{-3}), swellings (S) and folding endurance (folds) of PSS film and its composites

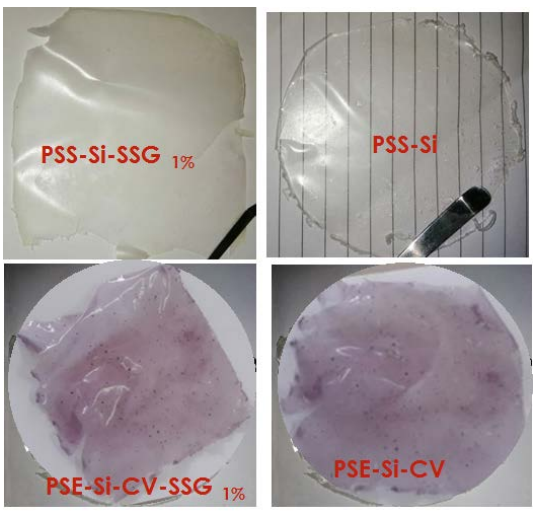

Figure 5. Visual aspect of selected films obtained from starch

3.4. Dye Characterization

Figure 6 displays the absorbance spectra of 12.5 x 10^{-6} $molL^{-1}$ crystal violet (CV, model drug) dissolved in chloroform at 37°C. It can be observed that the absorption spectra displayed the well-known structured band of the CV dye [70], giving a maximum absorption at about 580 nm and an extinction coefficient (ε) equal to 173155 M^{-1} cm^{-1}, the absorbance at maximum and ε were used to determine the amount of entrapped and released drug at 37°C , this temperature was selected in this study to mimic the body temperature.

3.5. Dye Entrapment and Release

The crystal violet entrapped in PSE-Si-CV and PSE-Si-CV-$SSG_{1\%}$ films was 20 and 38%, respectively. It was found that the drug entrapment markedly depended on the presence of SSG in the films. The amount of the CV entrapped in PSE-Si-CV-$SSG_{1\%}$ film was higher than that of PSE-Si-CV film. This could be because the electrostatic interaction of cationic dye (CV^+) was more with PSE-Si-CV-$SSG_{1\%}$ in comparison to PSE-Si-CV, since PSE-Si-CV-$SSG_{1\%}$ rich in anionic carboxylate moieties (COO^-) pendent in the SSG backbone.

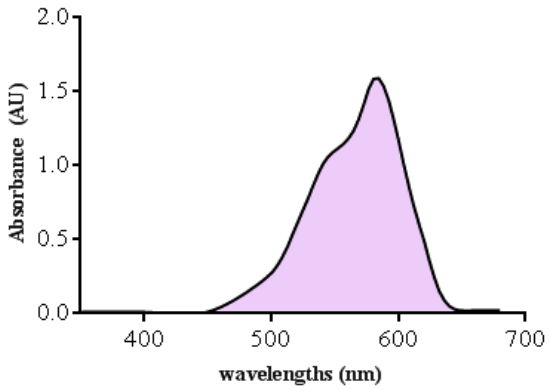

Figure 6. UV-vis absorption scan in a range equal to 350-650 nm for crystal violet (12.5 μM in chloroform) at 37°C

3.6. In-Vitro Release Study

The in vitro release of pure CV in PSE-CV and PSE-CV-$SSG_{1\%}$ physical mixtures reached approximately 10% after 300 min as displayed in Figure 7. Such a low releases is related to its low solubility and crystallinity of CV. On the other hand, the rate of CV release from films was significantly higher than that of the physical mixtures of CV (Figure 7). This large difference in dissolution rates could be attributed to the addition of plasticizer and the SSG polymer which enhance the water solubility and consequently the release rate from films. The CV release profiles in buffer solution (pH 7.4) 37°C is shown in Figure 7 for both films PSE-Si-CV and PSE-Si-CV-$SSG_{1\%}$. When compared with the high release rate for PSE-Si-CV because of adsorption sites which cover the surface of PSE are OH groups and at natural pH the starch chain is neutral as described in our previous work [42]. The OH groups of starch act as centers for interaction through forming hydrogen bonds with the cationic dye [71], for the PSE-Si-CV-$SSG_{1\%}$ film the CV release exhibited a weak tendency to be eliminated from the film.

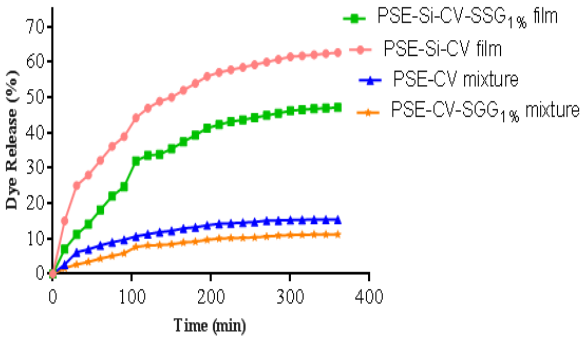

Figure 7. Release profiles of crystal violet from PSE-Si-CV film, PSE-Si-CV-SSG1% film, PSE-CV mixture and PSE-CV-SSG1% mixture in phosphate buffer solution (PBS) pH 7.4 at 37°C

This could be because CV was cationic, when it was incorporated and release from the anionic film (PSE-SSG), beside hydrogen bonding the electrostatic interaction may make a significant effect [72]. The CV and PSE-SSG film were oppositely charged, and so the electrostatic attraction existed between them and the dye strongly bonded in the film matrix, and the release amount of the PSE-Si-CV film was lower. These results are in agreement with Yue *et al.* [73] that investigated the effects of poly acrylic acid (PAA) content on the release efficiency of crystal violet from a film composed of PAA and poly vinyl alcohol (PVA), PAA and PVA have similar functional groups of PSE and SSG. It was found that the release rate of the drug decrease with increasing PAA content at 37°C.

3.7. Release Mechanisms

To specify the mechanism of model drug release, an *in-vitro* drug release profile was applied in four mathematical models and was interpreted in the form of graphical presentation as shown in Figure 8. Each model was assessed by correlation coefficient (R^2) as depicted in Table 3. The maximum value of correlation coefficient governs the appropriate mathematical model that tracks drug release kinetics [59]. Fitting of PSS-Si-CV and PSS-Si-CV-$SSG_{1\%}$ films experimental data recorded that Korsmeyer-Peppas and Higuchi model, exhibited higher degrees of correlation coefficient than other models. The drug release was properly fitted by Higuchi model (R^2 = 0.9308 for PSS-Si-CV and R^2 = 0.9556 for PSS-Si-CV-$SSG_{1\%}$), this suggests that release of model drug from films as a square root of time dependent process and diffusion controlled, slopes indicated that the PSE film had dissolution constant than PSS-Si-CV film, see Table 3. Furthermore, the Korsmeyer-Peppas model (R^2 = 0.9703for PSS-Si-CV and R^2 = 0.9626 for PSS-Si-CV-$SSG_{1\%}$) specified the kind of diffusion, which was evaluated by value, Release exponent (n = 0.4266 for PSS-Si-CV and n = 0.6078 for PSS-Si-CV-$SSG_{1\%}$) which suggests that the drug release from the PSS-Si-CV film follow quasi-Fickian diffusion mechanism, but for PSS-Si-CV-$SSG_{1\%}$ film obey to non-Fickian diffusion mechanism. Two mechanisms are represented in Scheme 1.

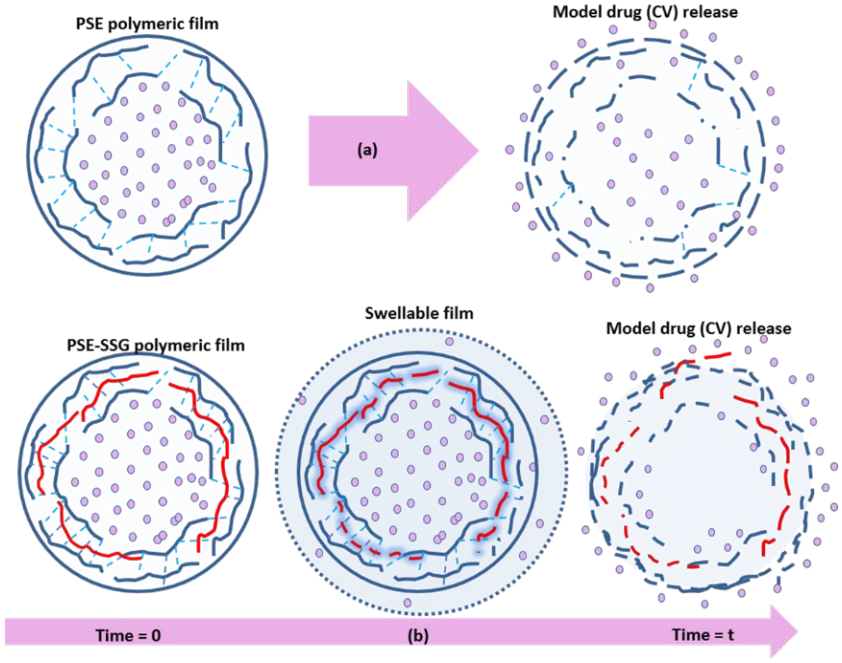

Scheme 1. Schematic representation of drug release from non swellable film-diffusion (a) and from a film made of swellable polymer (b). The phenomena of water uptake, swelling, polymer chain relaxation, drug diffusion, polymer chain disentanglement, and polymer edibility are depicted

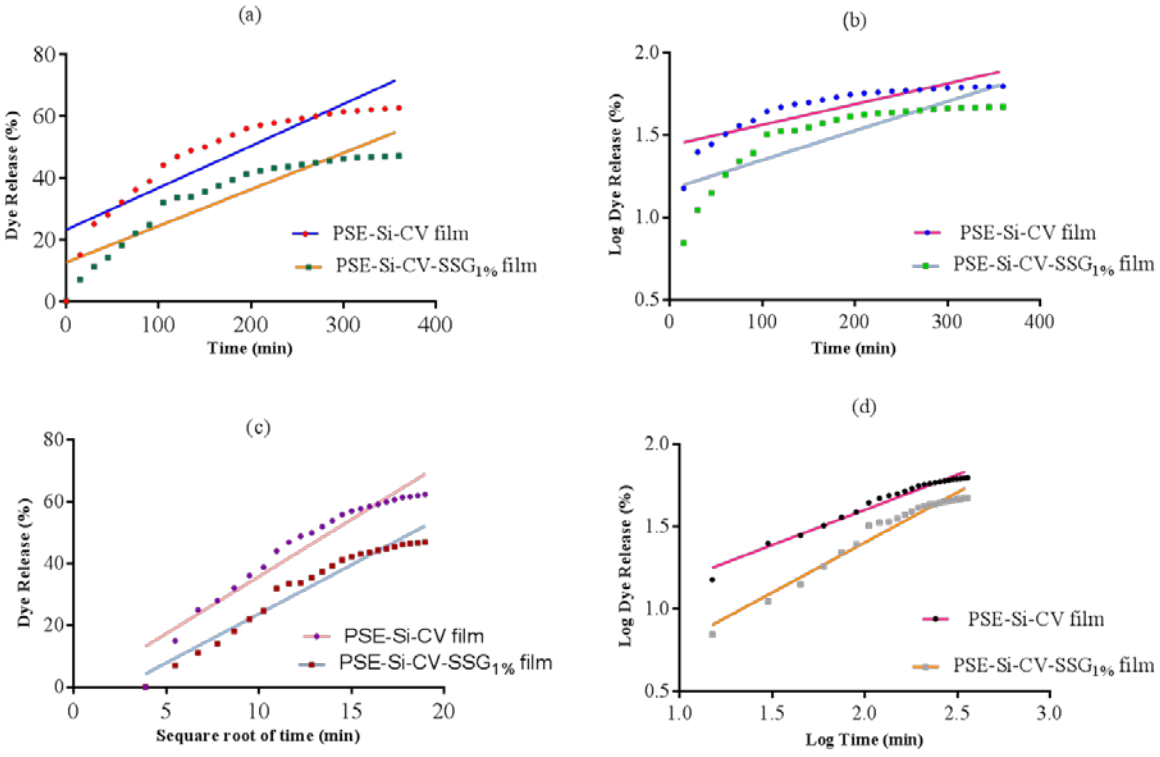

Figure 8. Zero order (a), first order (b), Higuchi model, (c), and Korsmeyer-Peppas model (d) kinetics release of CV from PSE-Si-CV and PSE-Si-CV-SSG$_{1\%}$ films in phosphate buffer solution (PBS) pH 7.4 at 37°C

Table 3. Results of different models in terms of R^2, slope and intercept of CV release from PSE-Si-CV and PSE-Si-CV-SSG films in phosphate buffer solution (PBS) pH 7.4 at 37°C

Mathematical fit	PSE-Si-CV film			PSE-Si-CV-SSG film		
	Slope	Intercept	R^2	Slope	Intercept	R^2
Zero order model	0.1359	23.21	0.8123	0.1185	12.58	0.8562
First order model	0.0013	1.438	0.7274	0.0018	1.172	0.7122
Higuchi model	3.6980	-1.081	0.9308	3.1780	-7.997	0.9556
Korsmeyer-Peppas model	0.4266	0.7490	0.9703	0.6078	0.1883	0.9626

4. Conclusions

Starch was extracted from potato in pure form and its physicochemical properties was close to commercial starches. A series of films of potato starch (PSS and PSE) blended with SSG and SiO_2 nanoparticles were successfully synthesized. The UV-vis spectra analysis showed that the PSS film had a lowest opacity values, increasing steadily with addition Si and intensely with adding of SSG. The UV barrier capacity of PSS films was increased by increasing the SSG content, but it was independent of silica concentration. Swelling properties of the films showed that the more the SSG content in the films, the higher the swelling ratio in various medium. Swelling ratio decreased with adding SiO_2 nanoparticles. Mechanical characteristics were related to the composition and swelling ratio of the films. Moreover, folding strength for PSS film was 100 folds which demonstrating good strength and elasticity, but incorporation of SSG and SiO_2 nanoparticles caused a marked reduction in folding endurance. Digital photograph exhibited a homogeneous structure, which indicated the good compatibility and miscibility between potato starch and SSG. Potential application of the PSE films in controlled drug delivery was also examined. The CV release from films was pointedly higher than that of the physical mixtures of CV in PSS and SSG powders in buffer solution at 37^{o}C. A lower release rate was observed for PSE-Si-CV-$SSG_{1\%}$ than that of PSE-Si-CV which was attributed to the electrostatic bonding existed between anionic SSG and the cationic dye (CV^{+}). The drug release mechanism is found to follow quasi-Fickian diffusion for the PSS-Si-CV film, but for PSS-Si-CV-$SSG_{1\%}$ film obey to non-Fickian diffusion mechanism.

Acknowledgements

We acknowledge the support from University of Benghazi (UOB).

Statement of Competing Interests

The Authors have no competing interests.

List of Abbreviations

Potato starch from Sigma-PSS
Potato starch extracted-PSE
Sodium starch glycolate-SSG
Ultraviolet Visible-UV-vis
Crystal violet-CV
Silica-Si
Phosphate buffer solution-PBS
Economic- eco
Carboxymethyl cellulose-CMC
Polyacrylic acid-PAA
Poly vinyl alcohol-PVA
Polyethylene-PE
Inductively coupled plasma mass spectrometry-ICP-MS
Polyacrylamide-PAM
Nanometer- nm
Centimeter- cm
Carr's index-CI
Swelling percent-S
Extinction coefficient-ε
Regression coefficient-R^2.

References

[1] Priya, B., Gupta, V. K., Pathania, D. and Singha, A. S., "Synthesis, characterization and antibacterial activity of biodegradable starch/pva composite films reinforced with cellulosic fibre,". *Carbohydrate polymers*, 109. 171-179. 2014.

[2] Bayor, M., Tuffour, E. and Lambon, P., "Evaluation of starch from new sweet potato genotypes for use as a pharmaceutical diluent, binder or disintegrant," *Journal of applied pharmaceutical science*, 3. S17-S23. 2013.

[3] Imam, S. H., "Stuck on starch: a new wood adhesive," *Agricultural research magazine*, 48. 1-9. 2000.

[4] Krishnan, P. G., Julson, J. L., Robison, D. J. and Pathak Y. V., "Polyethylene-starch extrudates as erodible carriers for bioactive materials: I. Erodibility and in vitro dye release studies," *Journal of biomaterials applications*, 8. 285-297. 1994.

[5] Ojogbo, E., Ogunsona, E. O. and Mekonnen, T. H., "Chemical and physical modifications of starch for renewable polymeric materials," *Materials today sustainability*, 100028. 2019.

[6] Passaretti, M., Ninago, M., Paulo, C., Petit, H., Irassar, E., Vega, D., Villar M. and Lez, O. V., "Biocomposites based on thermoplastic starch and granite sand quarry waste," *Journal of renewable materials*, 7. 393-402. 2019.

[7] Shahriari, T. and NabiBidhendi, G., "Starch efficiency in water turbidity removal," *Asian journal of natural & applied sciences*, 1. 34-37. 2012.

[8] Shalviri, A., Liu, Q., Abdekhodaie, M. J. and Wu. X. Y., "Novel modified starch-xanthan gum hydrogels for controlled drug delivery: Synthesis and characterization," *Carbohydrate polymers*, 79. 898-907. 2010.

[9] Silva, O. A., Pellá, M. G., Pellá, M. G., Caetano, J., Simões, M. R., Bittencourt, P. R. S. and Dragunski, D. C., "Synthesis and characterization of a low solubility edible film based on native cassava starch," *International journal of biological macromolecules*, 128. 290-296. 2019.

[10] Spychaj, T., zdanowicz, M., kujawa, J. And Schmidt, B., "Carboxymethyl starch with high degree of substitution synthesis, properties and application," *Polimery*, 58. 501-630. 2013.

[11] Suderman, N., Sarbon, N. and Mohamad Isa, M. I. N., "Effect of drying temperature on the functional properties of biodegradable cmc-based film for potential food packaging," *International food research journal*, 23. 1075-1084. 2016.

[12] Kim, M. and Pometto 3rd, A. L., "Food packaging potential of some novel degradable starch-polyethylene plastics (1)," *Journal of food protection*, 57. 1007-1012. 1994.

[13] Belay, Z. and Emire, S., "Development and characterization of antimicrobial packaging films," *Journal of food processing and technology*, 4. 000235. 2013.

[14] Sadeghizadeh-Yazdi, J., Habibi, M., Kamali, A. and Banaei, M., "Application of edible and biodegradable starch-based films in food packaging: A systematic review and meta-analysis," *Current research in nutrition and food science journal*, 7. 624-637. 2019.

[15] Lawton, J. W., "Effect of starch type on the properties of starch containing film," *Carbohydrate polymers*, 29. 203-208. 1996.

[16] Mehyar, G. and Han, J., "Physical and mechanical properties of high ‐ amylose rice and pea starch films as affected by relative humidity and plasticizer," *Journal of food science*, 69. E449-E454. 2006.

[17] Zhang, S., Wei, F. and Han, X., "An edible film of sodium alginate/pullulan incorporated with capsaicin," *New journal of chemistry*, **4**2. 17756-17761. 2018.

[18] Rosseto, M., Krein, D., Balbé, N. and Dettmer, A., "Starch ‐ gelatin film as an alternative to the use of plastics in agriculture - a review," *Journal of the science of food and agriculture*, 99. 2019.

[19] Chang, Q., Hao, Y., Cheng, L., Liu Y. and Qu, A., "Preparation and performance evaluation of biodegradable corn starch film

using poly (lactic acid) as waterproof coating," *Surface engineering*, 1-6. 2019.

[20] Huo, W., Xie, G., Zhang, W., Wang, W., Shan, J., Liu, H. and Zhou, X., "Preparation of a novel chitosan-microcapsules/starch blend film and the study of its drug-release mechanism," *International journal of biological macromolecules*, 87. 114-122. 2016.

[21] Ismail, H. and Zaaba, N. F., "The mechanical properties, water resistance and degradation behaviour of silica-filled sago starch/pva plastic films," *Journal of elastomers & plastics*, 46. 96-109. 2012.

[22] Krogars, K., Heinämäki, J., Karjalainen, M., Niskanen, A., Leskelä, M. and Yliruusi, J., "Enhanced stability of rubbery amylose-rich maize starch films plasticized with a combination of sorbitol and glycerol," *International journal of pharmaceutics*, 251. 205-8. 2003.

[23] Tang, H., Xiong, H., Tang, S. and Zou, P., "A starch-based biodegradable film modified by nano silicon dioxide," *Journal of applied polymer science*, 113. 34-40. 2009.

[24] Wolff I., A., Davis, H. A., Cluskey, J. E., Gundrum L. J. and Rist, C. E., "Preparation of films from amylose," *Industrial & engineering chemistry*, 43. 915-919. 1951.

[25] Rankin, J., Wolff, I., Davis, H. and Rist, C., "Permeability of amylose film to moisture vapor, selected organic vapors, and the common gases," *Industrial & engineering chemistry chemical & engineering data series*, 3. 120-123. 1958.

[26] Zhang, R., Wang, X. and Cheng, M., "Preparation and characterization of potato starch film with various size of nano-SiO_2," *Polymers*, 10. 1172. 2018.

[27] And, Z. and Han, J., "Film-forming characteristics of starches," *Journal of food science*, 70. E31-E36. 2005.

[28] López, O. V., Ninago, M. D., Lencina, M. M. S., García, M. A., Andreucetti, N. A., Ciolino, A. E. and Villar, M. A., "Thermoplastic starch plasticized with alginate-glycerol mixtures: Melt-processing evaluation and film properties," *Carbohydrate polymers*, 126. 83-90. 2015.

[29] Perry, P. A. and Donald, A., "The role of plasticization in starch granule assembly," *Biomacromolecules*, 1. 424-32. 2000.

[30] Bertuzzi, M., Gottifredi, J. and Armada, M., "Mechanical properties of a high amylose content corn starch based film, gelatinized at low temperature," *Brazilian journal of food technology*, 15. 219-227. 2012.

[31] Rahmah, M., Mohd, N., Norizan. M. N., Aisyah, M. and Fauzi, F., "Swelling and tensile properties of starch glycerol system with various crosslinking agents," *IOP conference series: materials science and engineering*, 223. 012059. 2017.

[32] Zavareze, E., Zanella, Pinto, V., Klein, B., Halal, S., Elias, M., Prentice, C. and Dias, Á., "Development of oxidised and heat-moisture treated potato starch film," *Food chemistry*, 132. 2011.

[33] Shogren, R. L., Greene, R. V. and WU, Y. V., "Complexes of starch polysaccharides and poly(ethylene co-acrylic acid): Structure and stability in solution," *Journal of applied polymer science*, 42. 1701-1709. 1991.

[34] Sarwono, A., Man, Z., Bustam, M. A., Subbarao, D., Idris, A., Muhammad, N., Khan, A. S. and Ullah, Z., "Swelling mechanism of urea cross-linked starch-lignin films in water," *Environmental technology*, 39. 1522-1532. 2018.

[35] Suriyatem, R., Auras, R. A. and Rachtanapun, P., "Improvement of mechanical properties and thermal stability of biodegradable rice starch-based films blended with carboxymethyl chitosan," *Industrial crops and products*, 122. 37-48. 2018.

[36] Almasia, H., Ghanbarzadeha, B. and Entezami, A. A., "Physicochemical properties of starch-cmc-nanoclay biodegradable films," *International journal of biological macromolecules*, 46. 1-5. 2010.

[37] Sheskey, P. J., Cook, W. G. and Cable, C. G., *Handbook of pharmaceutical excipients*, Pharmaceutical Press, London, 2017.

[38] Xie J., Luo, Y., Liu, Y., Ma, Y., Yue, P. and Yang, M., "Novel redispersible nanosuspensions stabilized by co-processed nanocrystalline cellulose-sodium carboxymethyl starch for enhancing dissolution and oral bioavailability of baicalin," *International journal of nanomedicine*, 14. 353-369. 2019.

[39] Eltaboni, F. and Imragaa, A., "Physical and chemical modifications of starches," *In 'proceeding of 2nd Libyan conference on chemistry and its applications*, 1. 120-123. 2017.

[40] Eltaboni, F., Caseley, E., Katsikogianni, M., Swanson, L., Swift, T. and Romero-Gonzalez, M., "Fluorescence spectroscopy analysis of the bacteria-mineral interface: Adsorption of lipopolysaccharides to silica and alumina," *Langmuir*, 36, 1623-1632. 2020.

[41] Eltaboni, F., Imragaa, A., Alzintani, W. and Almograbi, H., "Kinetic study of macromolecular interaction of starch onto silica nanoparticles," *In 'proceeding of 2nd Libyan conference on chemistry and its applications*, 2. 87-89. 2018.

[42] Eltaboni, F., Imragaa, A., Edbey, K., Elabdily, K. and Mousa, N., "Adsorption and conformations of starch at solid-liquid interfaces using spectrophotometry and turbidity techniques," *American chemical science journal*, 9.1-11. 2015.

[43] Tang, H., Xiong, H., Tang, S. and Zou, P., "A starch-based biodegradable film modified by nano silicon dioxide," *Journal of applied polymer science*, 113. 34-40. 2009.

[44] Shi, X., Hassanzadeh-Aghdam, M. K. and Ansari, R., "Viscoelastic analysis of silica nanoparticle-polymer nanocomposites," *Composites part B: engineering*, 158. 169-178. 2019.

[45] Yang, J., Han, C., Duan, J.-F., Xu, F. and Sun, R.-C., "Interaction of silica nanoparticle/polymer nanocomposite cluster network structure: revisiting the reinforcement mechanism," *The journal of physical chemistry* C, 117. 8223-8230. 2013.

[46] Xie, Y., Yan, M., Yuan, S., Sun, S. and Huo, Q. J. C. C. J., "Effect of microwave treatment on the physicochemical properties of potato starch granules," *Chemistry central journal*, 7. 1-7. 2013.

[47] Wuttisela, K., Shobsngob, S. and Triampo, W., "Amylose/amylopectin simple determination in acid hydrolyzed tapioca starch," *Journal of the chilean chemical society - J CHIL CHEM SOC*, 53. 1565-1567. 2008.

[48] Jonhed, A. and Järnström, L., "Phase and gelation behavior of 2-hydroxy-3-(n, n-dimethyl-n-dodecylammonium) propyloxy starches," *Starch / stärke*, 55. 569-575. 2003.

[49] Wyatt, P. J., "Measurement of special nanoparticle structures by light scattering," *Analytical chemistry*, 86. 7171-7183. 2014.

[50] Sinko, P. J. and Martin, A. N., *Martin's physical pharmacy and pharmaceutical sciences: Physical chemical and biopharmaceutical principles in the pharmaceutical sciences*, Lippincott Williams & Wilkins, Philadelphia, 2006.

[51] Obitte, N. and Chukwu, A., "Preliminary studies on tacca involucrata (schum & thonn) starch. Fam_ taccaceae," *West african journal of pharmacy*, 20. 8-13. 2007.

[52] Koc, B., Sakin-Yilmazer, M., Kaymak-Ertekin, F. and Balkir, P., "Physical properties of yoghurt powder produced by spray drying," *Jouranl of food science and technolgy*, 51. 1377-1383. 2014.

[53] Carr, R. L., "Evaluating flow properties of solids Chemical," *Engineering*, 72. 163-168. 1965.

[54] Souza, A. C., Benze, R., Ferrão, E. S., Ditchfield, C., Coelho, A. C. V. and Tadini, C. C., "Cassava starch biodegradable films: Influence of glycerol and clay nanoparticles content on tensile and barrier properties and glass transition temperature," *LWT - food science and technology*, 46. 110-117. 2012.

[55] de Moraes, J. O., Müller, C. M. O. and Laurindo, J. B., "Influence of the simultaneous addition of bentonite and cellulose fibers on the mechanical and barrier properties of starch composite-films,"*Food science and technology international*, 18. 35-45, 2012.

[56] Zayed, G. M., Rasoul, S. A.-E., Ibrahim, M. A., Saddik, M. S. and Alshora, D. H.: "In vitro and in vivo characterization of domperidone-loaded fast dissolving buccal films," *Saudi pharmaceutical journal*, 28. 266-273. 2020.

[57] Nair, S. B. and Jyothi, A. N., "Cassava starch-konjac glucomannan biodegradable blend films: In vitro study as a matrix for controlled drug delivery," *Starch/stärke*, 65. 273-284. 2013.

[58] Dash, S., Murthy, P. N., Nath, L. and Chowdhury, P., "Kinetic modeling on drug release from controlled drug delivery systems," *Acta poloniae pharmaceutica*, 67. 217-23. 2010.

[59] Baishya, H., "Application of mathematical models in drug release kinetics of carbidopa and levodopa er tablets," *Journal of developing drugs*, 06. 2017.

[60] Onunkwo, G. and Onyishi, I., "Kinetics and mechanisms of drug release from swellable and non swellable matrices: A review," *Research journal of pharmaceutical, biological and chemical sciences*, 4. 97-103. 2013.

[61] Olejnik, A., Kapuscinska, A., Schroeder, G. and Nowak I., "Physico-chemical characterization of formulations containing endomorphin-2 derivatives," *Amino acids*, 49. 1719-1731. 2017.

[62] Paarakh, M. P., Jose, P. A., Setty, C. and Christoper P., "Release kinetics-concepts and applications," *International journal of pharmacy research & technology*, 10. 1-9. 2018.

[63] Theisen, A., Johann, C., Deacon, M. P. and Harding S. E., *Refractive increment data-book for polymer and biomolecular scientists*, Nottingham University Press, Nottingham, 2000.

[64] Stojanović, Ž. P., Jeremić, K., Jovanović, S., Nierling, W. and Lechner, M. D., "Light scattering and viscosity investigation of dilute aqueous solutions of carboxymethyl starch," *Starch/stärke*, 61. 199-205. 2009.

[65] Commission, B. P.: *British pharmacopoeia 2007*. Stationery Office, 2006.

[66] Bonsu, M. A., Ofori-Kwakye, K., Kipo, S. L., Boakye-Gyasi, M. E. and Fosu M.-A., "Development of oral dissolvable films of diclofenac sodium for osteoarthritis using albizia and khaya gums as hydrophilic film formers," *Journal of drug delivery*, 2016. 6459280. 2016.

[67] Wahyuningtyas, D. and Dinata A., "Combination of carboxymethyl cellulose (cmc) - corn starch edible film and glycerol plasticizer as a delivery system of diclofenac sodium," *In 'AIP conference proceedings' 1977*, 030032-1-030032-8. 2018.

[68] Wilpiszewska, K., "Hydrophilic films based on starch and carboxymethyl starch," *Polish journal of chemical technology*, 21. 26-30. 2019.

[69] Semalty, A., Semalty, M., Nautiyal, U., "Formulation and evaluation of mucoadhesive buccal films of enalapril maleate," *Indian journal of pharmaceutical sciences*, 72. 571-575. 2010.

[70] Al-Kadhemy, M., "Absorption spectrum of crystal violet in chloroform solution and doped PMMA thin films," *Atti della fondazione giorgio ronchi*, 3. 359. 2012.

[71] Amiri, M. J., "Optimization of crystal violet adsorption by chemically modified potato starch using response surface methodology," *Pollution*, 6. 159-170. 2020.

[72] Lin, J., Li D., Chen, P., Wang, J. and Xu, S., "Interaction between carboxymethyl starch and cetyl trimethylammonium bromide," *Chemistry bulletin / huaxue tongbao*, 74. 1131-1134+1139. 2011.

[73] Yue, Y.-M., Xu K., Liu, X.-G., Chen, Q., Sheng, X. and Wang, P.-X., "Preparation and characterization of interpenetration polymer network films based on poly(vinyl alcohol) and poly(acrylic acid) for drug delivery," *Journal of applied polymer science*, 108. 3836-3842. 2008.